

Imaging of the 3D dynamics of flagellar beating in human sperm.

Silva-Villalobos¹, F., Pimentel, J.A.², Darszon, A.³, Corkidi, G.⁴.

Abstract—The study of the mechanical and environmental factors that regulate a fundamental event such as fertilization have been subject of multiple studies. Nevertheless, the microscopical size of the spermatozoa and the high beating frequency of their flagella (up to 20 Hz) impose a series of technological challenges for the study of the mechanical factors implicated. Traditionally, due to the inherent characteristics of the rapid sperm movement, and to the technological limitations of microscopes (optical or confocal) to follow in three dimensions (3D) their movement, the analysis of their dynamics has been studied in two dimensions, when the head is confined to a surface. Flagella propel sperm and while their head can be confined to a surface, flagellar movement is not restricted to 2D, always displaying 3D components. In this work, we present a highly novel and useful tool to analyze sperm flagella dynamics in 3D. The basis of the method is a 100 Hz oscillating objective mounted on a bright field optical microscope covering a 16 microns depth space at a rate of ~ 5000 images per second. The best flagellum focused subregions were associated to their respective Z real 3D position. Unprecedented graphical results making evident the 3D movement of the flagella are shown in this work and supplemental material illustrating a 3D animation using the obtained experimental results is also included.

I. INTRODUCTION

The quantitative analysis of the dynamic behavior associated to the movement of tubular structures in biological samples plays an important role in many different circumstances: from the study of neurite dynamic growth to the analysis of the beat patterns of cilia and flagella (structural appendages of eukaryotic cells) involved in embryological development in many vertebrate species [1], [2], [3]. In this sense, developing imaging tools to determine biological sample dynamics becomes a relevant topic for the computer vision field. Under these considerations, this work proposes a three dimensional (3D) imaging system oriented to acquire and analyze human sperm flagellar dynamics and its

implications in human sperm swimming towards the egg fertilization. Traditionally, due to the inherent characteristics of the rapid sperm movement (mammals or marine species), and to the technological limitations of microscopes (optical or confocal) to follow in 3D their movement, the analysis of their dynamics has been studied in two dimensions, when the cell swims confined to a surface. In this way, while the movement of a free 3D swimming sperm shows helical patterns (for some marine species for example), when swimming confined to a surface, its movement becomes circular. Flagella propel sperm and while their head can be confined to a surface, flagellar movement is not restricted to 2D, always displaying 3D components. Our experimental evidence supports this idea, namely that small sperm flagella subregions move slightly out of focus when they are beating near a surface (Fig. 1 and Fig. 2), (see also Guerrero *et al.* [4]). Traditionally this movement has been simplified to a 2D movement losing the details of its real three dimensional beating.

To deal with this challenge, it is a fact that the sperm flagella is a tubular structure and multiple proposed works examining microscopical tubular information have been developed [5], [6], [7]. In this sense, Al-Kofahi *et al.* [8] designed an algorithm to search linear structures based into a recursive process that, seeded by manually designed initial points, grow and fit a piece wise linear structure. In 2004, Meijering *et al.* [9] proposed an algorithm, using a minimal criteria defined in terms of second order directional derivatives, looking for the path of minimal cost between an initial and final point. Given that this criteria exhibit high sensitivity to environment factors like low contrast data, a series of improvements were proposed in further works. For example, Zhang *et al.* [10] incorporated an automatic process to determine the endpoint and other works including the management of non-uniform backgrounds and noise minimization [11], [12], [13].

*This work was supported by the Dirección General de Asuntos del Personal Académico; by the Universidad Nacional Autónoma de México (DGAPA-UNAM) grant IN225406-3 to A. Darszon; and by the Consejo Nacional de Ciencia y Tecnología (CONACYT) grant 39908-Q to A. Darszon; and by CONACYT M.Sc. scholarship to F. Silva-Villalobos.

¹ F. Silva-Villalobos is with the Computational Modelling and Scientific Computing Program, Universidad Autónoma del Estado de Morelos, 62200, Cuernavaca, Mexico. franksv@ibt.unam.mx

² J.A. Pimentel, is with National Laboratory of Advanced Microscopy, Institute of Biotechnology, Universidad Nacional Autónoma de México, 62200 Cuernavaca, Mexico. jarturo@ibt.unam.mx

³ A. Darszon, is with Institute of Biotechnology, Universidad Nacional Autónoma de México, 62200 Cuernavaca, Mexico. darszon@ibt.unam.mx

⁴ Corkidi, G. (corresponding author) is with Image and Computer Vision Laboratory, Institute of Biotechnology, Universidad Nacional Autónoma de México, 62200 Cuernavaca, Mexico. (phone: +52 777 3291710, corkidi@ibt.unam.mx)

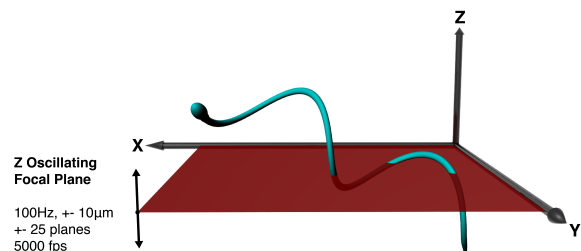


Fig. 1. Sperm flagella subregions move slightly out of focus depending on their 3D position. The focal plane of the objective oscillates at a frequency of 100 Hz while acquiring 5000 fps. The best focused points in each image give the 3D position of the flagella subregion.

In our case, it is important to consider that the human flagella beat frequency is typically $\sim 10\text{-}20$ Hz (typical head length of $5\ \mu\text{m}$ and a flagellum length $\sim 55\ \mu\text{m}$), though it depends on numerous factors such as media viscosity. These dynamic characteristics have constituted a major challenge concerning the analysis of the 3D sperm flagellar movement. To deal with these constrictions, we have taken as a basis an oscillating objective in a bright field microscope using a frequency that allows enough sampling of the flagella at different focal planes, as described in our earlier work dealing with the 3D+t tracking of sperm trajectories [14]. In this work, when stimulated by a triangular ramp, a piezoelectric device (mounted between a water immersion objective of an optical microscope and the turret) displaces the objective vertically at up to 100 cycles per second while a high speed camera acquires synchronously up to 5000 frames per second, capturing successive focal planes in a depth of $16\ \mu\text{m}$. Afterwards, the sperm heads were located automatically by detecting contrast inversion changes (as described in Pimentel *et al.* [15]). To segment the sperm flagella in 3Ds, we have associated the best flagellum focused subregions to their respective Z real 3D position (Fig. 2), as described in the following section. Unprecedented graphical results making evident the 3D movement of the flagella are shown in this work. Supplemental material showing a 3D animation using experimental results of the 3D movement of sperm flagella is also included. This method constitutes a highly novel and useful tool to analyze sperm flagella dynamics in 3D. The pre-processing procedure and semi-automatic segmentation and analysis of the image sequences are described in the next section.

II. MATERIAL AND METHODS

A. Biological preparations.

Human ejaculates were obtained from healthy donors by masturbation after at least 48 hours of sexual abstinence. In this work, the use of human sperm was approved by the Bioethics Committee of the Instituto de Biotecnología, Universidad Nacional Autónoma de México. Signed written informed consent forms were signed by all healthy donors. The human semen samples employed in this study fulfilled the requirements determined by the World Health Organization [16]. Highly motile sperm were recovered after a swim-up separation for 1 hour in Ham's F-10 medium at $37\ ^\circ\text{C}$ in a humidified atmosphere of $5\ \%$ CO_2 and $95\ \%$ air. For the experiments the cells were centrifuged 5 min at 3000 rpm and resuspended in physiological salt solutions at ~ 107 cells/ml. The physiological solution was in mM: 94 NaCl, 4 KCl, 2 CaCl₂, 1 MgCl₂, 1 Na-Piruvate, 25 NaHCO₃, 5 Glucose, 30 HEPES, 10 Lactate at pH 7.4.

B. Experimental device.

A piezoelectric device P-725 (Physik Instruments, MA, USA) was mounted between a 60X 1.00 NA water immersion objective (Olympus UIS-2 LUMPLFLN 60X W) and an inverted microscope Olympus IX71 (Fig. 3). This

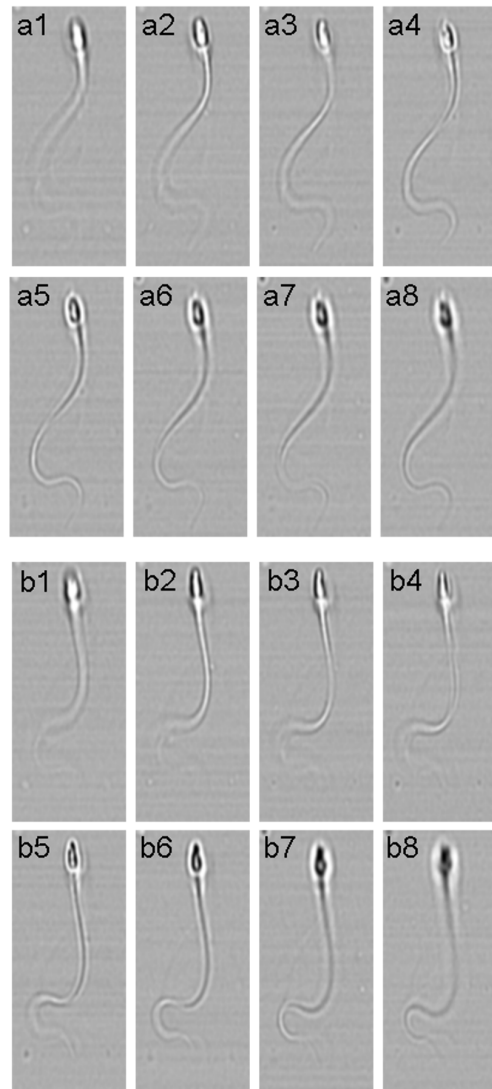


Fig. 2. Two image sequences (a1-8, b1-8) of a real human spermatozoa at successive focal planes, at two different moments, showing how flagella subregions get in/out of focus, evidencing the 3D movement of the sperm flagella.

piezoelectric device was controlled by a servo-controller E-501 via a high current amplifier E-505 (Physik Instruments, MA, USA). The servo-controller was excited with a ramp signal from the E-506 function generator. A synchronizing TTL pulse coming from the servo-controller was used for triggering the high speed camera Optronis 5000X BW with 4 Gigabyte RAM (for grabbing up to 3.2 seconds image sequences of 512×512 pixels; in our case 5,000 images per second). The microscope was mounted on an optical table (TMC) to isolate the system from external vibrations. The system includes a thermal controller (Warner Instruments TCM/CL-100) to preserve the optimal conditions of biological preparations. Data acquisition and tracking was achieved with a Pentium IV PC (1.8 GHz) (details in Corkidi *et al.* [14], Pimentel *et al.* [15]).

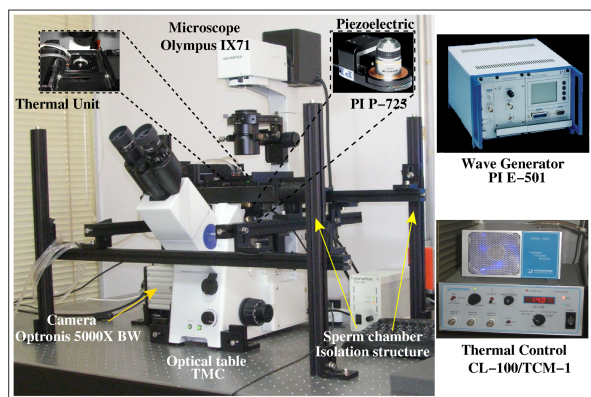


Fig. 3. Experimental set designed to acquire the 3D information of the spermatozoa displacement including its flagellar beating [17].

C. Flagella tracking.

A flow diagram describing the steps for processing and obtaining the 3D data of the flagellar beating of the human sperm is shown in Fig. 4.

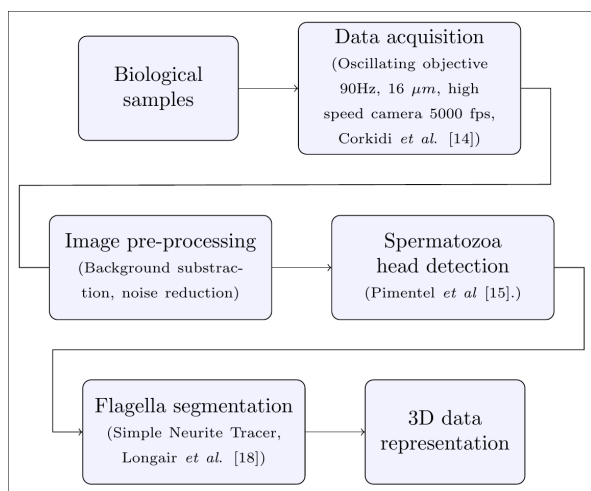


Fig. 4. The flow diagram describes the whole process designed to obtain the flagellar beating dynamics related to a sperm swimming in a three dimensional space.

1) *Pre-processing*: Designed to minimize image noise and enhance contrast between object (flagella) and background. The process starts by the subtraction of the background (defined as the average component of the entire stack) from each one of the images into the stack. Then, a low pass Fourier Filter is applied to minimize the electronic noise coming from the CCD camera sensor and finally, an equalization process over the histogram is applied. The result is a stack with a uniform background without high frequency noise.

2) *Head detection and flagella segmentation*: The analysis of the sperm movement dynamics in 3D requires first head detection and position determination while cells are moving. Previously we presented an original segmentation algorithm taking advantage of the 3D characteristic diffrac-

tion pattern associated to the sperm head to determine its three dimensional position [15]. Based on these results, from a collection of 3D trajectories, each point of each trajectory (corresponding to the instantaneous sperm head position) can be used as the seed point of the flagella segmentation procedure. Considering this, we included in our pipe-line analysis the open source utility called Simple Neurite Tracer, developed by Longair *et al.* [18]. This utility allows building a simple 3D path between successive points along the mid-line of a neural process. The interface includes the ability to create branches from the original paths, tree structures or even cyclic topologies. In this work, the constitutive points of the trajectory are linked using the algorithm A^* proposed by Hart *et al.* [19] and based on the criteria developed by Wink *et al.* [20] where it is involved the cost of moving to a new point. To improve the convergence velocity of the algorithm, this methodology can be combined with a Hessian surface mapping of the curvature and with criterias of size and shape (Sato *et al.* [21]). A more elaborated methodology based on multi-scale filtering can be implemented (Frangi *et al.* [22]).

III. RESULTS.

The Fig. 5 shows, for a single sperm, three different perspectives of the dynamical behavior described by its flagella at different consecutive cycles. An interesting facts is that despite the head of the selected spermatozoa is constrained to the glass surface of the container (flat bottom), the flagella movement shows an evident and complex three dimensional movement. An animation of this movement can be observed at http://www.ibt.unam.mx/labimage/proyectos.php?lang=spa&id=13&watch=ok&video=fotos_proyectos/Originales_DAT_Animacion.flv. These unprecedented results show that the spatial and temporal resolution reached by our system is enough to explore the complex dynamical behavior of the flagella movement. Considering that the flagella movement is a primary indicator of the intracellular mechanisms employed by the cells to reorientate its swim in response to specific chemical stimuli, the proposed imaging system offers promising perspectives concerning the analysis of the effects that the environmental conditions imposes on the sperm movement and consequently over one of the major components dealing with fertilization success. Technically, this imaging system, constitutes the basis for a deeper understanding of the free swimming of flagellated cells, nevertheless there exists several opportunities to improve the information acquisition, for example, a more automated version is required to make possible a greater number of sperm samples for a statistical analysis of different experimental conditions. This include the development of high throughput platforms including the implementation of *graphics processing units* (GPU's) based algorithms.

ACKNOWLEDGMENTS

We thank Esperanza Mata (PCB/UNAM) for her helpful assistance with the biological experimental procedure.

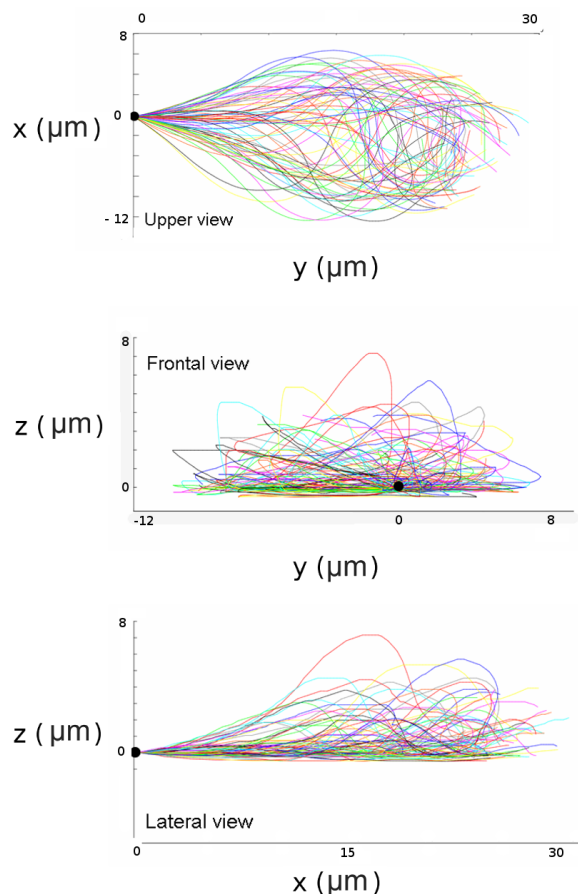


Fig. 5. Consecutive 3D human sperm flagellar forms, upper, frontal and lateral views. The graphs show a single spermatozoa flagella for 76 sequential cycles. The black dot represents the sperm head position.

REFERENCES

- [1] L. G. Wilson, L. M. Carter, and S. E. Reece, "High-speed holographic microscopy of malaria parasites reveals ambidextrous flagellar waveforms," *Proceedings of the National Academy of Sciences*, vol. 110, no. 47, pp. 18769–18774, 2013. [Online]. Available: <http://www.pnas.org/content/110/47/18769.abstract>
- [2] I. H. Riedel-Kruse, A. Hilfinger, J. Howard, and F. Jülicher, "How molecular motors shape the flagellar beat," *HFSP Journal*, vol. 1, no. 3, pp. 192–208, 2007, PMID: 19404446. [Online]. Available: <http://www.tandfonline.com/doi/abs/10.2976/1.2773861>
- [3] A. Hilfinger, "Dynamics of cilia and flagella," Ph.D. dissertation, Ph. D. dissertation, TU Dresden, 2006.
- [4] A. Guerrero, J. Carneiro, A. Pimentel, C. D. Wood, G. Corkidi, and A. Darszon, "Strategies for locating the female gamete: the importance of measuring sperm trajectories in three spatial dimensions," *Molecular Human Reproduction*, vol. 17, no. 8, pp. 511–523, 2011. [Online]. Available: <http://molehr.oxfordjournals.org/content/17/8/511.abstract>
- [5] D. E. Donohue and G. A. Ascoli, "Automated reconstruction of neuronal morphology: An overview," *Brain Research Reviews*, vol. 67, no. 1–2, pp. 94–102, 2011. [Online]. Available: <http://www.sciencedirect.com/science/article/pii/S0165017310001293>
- [6] C. Wu, J. Schulte, K. Sepp, J. Littleton, and P. Hong, "Automatic Robust Neurite Detection and Morphological Analysis of Neuronal Cell Cultures in High-content Screening," *Neuroinformatics*, vol. 8, no. 2, pp. 83–100. [Online]. Available: <http://dx.doi.org/10.1007/s12021-010-9067-9>
- [7] E. Meijering, "Neuron tracing in perspective," *Cytometry Part A*, vol. 77, no. 7, pp. 693–704, 2010.
- [8] K. Al-Kofahi, S. Lasek, D. Szarowski, C. Pace, G. Nagy, J. Turner, and B. Roysam, "Rapid automated three-dimensional tracing of neurons from confocal image stacks," *Information Technology in Biomedicine, IEEE Transactions on*, vol. 6, no. 2, pp. 171–187, June 2002.
- [9] E. Meijering, M. Jacob, J.-C. Sarria, P. Steiner, H. Hirling, and M. Unser, "Design and validation of a tool for neurite tracing and analysis in fluorescence microscopy images," *Cytometry Part A*, vol. 58A, no. 2, pp. 167–176, 2004. [Online]. Available: <http://dx.doi.org/10.1002/cyto.a.20022>
- [10] Y. Zhang, X. Zhou, A. Degterev, M. Lipinski, D. Adjeroh, J. Yuan, and S. T. Wong, "Automated neurite extraction using dynamic programming for high-throughput screening of neuron-based assays," *NeuroImage*, vol. 35, no. 4, pp. 1502–1515, 2007. [Online]. Available: <http://www.sciencedirect.com/science/article/pii/S1053811907000444>
- [11] M. L. Narro, F. Yang, R. Kraft, C. Wenk, A. Efrat, and L. L. Restifo, "NeuronMetrics: Software for semi-automated processing of cultured neuron images," *Brain Research*, vol. 1138, no. 0, pp. 57–75, 2007. [Online]. Available: <http://www.sciencedirect.com/science/article/pii/S000689930603215X>
- [12] P. J. Broser, S. Erdogan, V. Grinevich, P. Osten, B. Sakmann, and D. J. Wallace, "Automated axon length quantification for populations of labelled neurons," *Journal of Neuroscience Methods*, vol. 169, no. 1, pp. 43–54, 2008. [Online]. Available: <http://www.sciencedirect.com/science/article/pii/S0165027007005894>
- [13] M. Pool, J. Thiemann, A. Bar-Or, and A. E. Fournier, "NeuriteTracer: A novel ImageJ plugin for automated quantification of neurite outgrowth," *Journal of Neuroscience Methods*, vol. 168, no. 1, pp. 134–139, 2008. [Online]. Available: <http://www.sciencedirect.com/science/article/pii/S016502700700430X>
- [14] G. Corkidi, B. Taboada, C. Wood, A. Guerrero, and A. Darszon, "Tracking sperm in three-dimensions," *Biochemical and Biophysical Research Communications*, vol. 373, no. 1, pp. 125–129, 2008. [Online]. Available: <http://www.sciencedirect.com/science/article/pii/S0006291X08011236>
- [15] J. Pimentel, J. Carneiro, A. Darszon, and G. Corkidi, "A segmentation algorithm for automated tracking of fast swimming unlabelled cells in three dimensions," *Journal of Microscopy*, vol. 245, no. 1, pp. 72–81, 2012. [Online]. Available: <http://dx.doi.org/10.1111/j.1365-2818.2011.03545.x>
- [16] T. G. Cooper, E. Noonan, S. von Eckardstein, J. Auger, H. G. Baker, H. M. Behre, T. B. Haugen, T. Kruger, C. Wang, M. T. Mbizvo, and K. M. Vogelsong, "World Health Organization reference values for human semen characteristics," *Human Reproduction Update*, vol. 16, no. 3, pp. 231–245, 2010. [Online]. Available: <http://humupd.oxfordjournals.org/content/16/3/231.abstract>
- [17] A. Pimentel and G. Corkidi, "Mechanical vibration compensation method for 3D+t multi-particle tracking in microscopic volumes," in *Engineering in Medicine and Biology Society, 2009. EMBC 2009. Annual International Conference of the IEEE*, Sept 2009, pp. 1429–1432.
- [18] M. H. Longair, D. A. Baker, and J. D. Armstrong, "Simple Neurite Tracer: Open Source software for reconstruction, visualization and analysis of neuronal processes," *Bioinformatics*, 2011.
- [19] P. Hart, N. Nilsson, and B. Raphael, "A Formal Basis for the Heuristic Determination of Minimum Cost Paths," *Systems Science and Cybernetics, IEEE Transactions on*, vol. 4, no. 2, pp. 100–107, July 1968.
- [20] O. Wink, W. Niessen, and M. Viergever, "Minimum cost path determination using a simple heuristic function," in *Pattern Recognition, 2000. Proceedings. 15th International Conference on*, vol. 3, 2000, pp. 998–1001 vol.3.
- [21] Y. Sato, S. Nakajima, N. Shiraga, H. Atsumi, S. Yoshida, T. Koller, G. Gerig, and R. Kikinis, "Three-dimensional multi-scale line filter for segmentation and visualization of curvilinear structures in medical images," *Medical Image Analysis*, vol. 2, no. 2, pp. 143–168, 1998. [Online]. Available: <http://www.sciencedirect.com/science/article/pii/S1361841598800091>
- [22] A. F. Frangi, W. Niessen, K. Vincken, and M. Viergever, "Multiscale vessel enhancement filtering," in *Medical Image Computing and Computer-Assisted Intervention — MICCAI'98*, ser. Lecture Notes in Computer Science, W. Wells, A. Colchester, and S. Delp, Eds. Springer Berlin Heidelberg, vol. 1496, pp. 130–137. [Online]. Available: <http://dx.doi.org/10.1007/BF0056195>